


## Adaptive Resilient Control of Grid-Forming Converters for High-Renewable Transmission Networks

Rio Khalifa

Pembangunan Panca Budi University, Medan, Indonesia

Article Info	ABSTRACT
<p><b>Keywords:</b> Grid-forming converters (GFC); Adaptive control; Resilient control; Effective short-circuit ratio (eSCR); Virtual synchronous machine (VSM); Droop control; Impedance shaping; Angle-aware current limiting; Fault ride-through (FRT); Low-SCR grids; Multi-GFC coordination; Passivity &amp; ISS stability.</p>	<p>High renewable penetration makes the transmission grid inertia-light and vulnerable to frequency/voltage deviations, interconverter resonances, and current limits during disturbances. This paper proposes an Adaptive-Resilient Grid-Forming Converter (AR-GFC) that integrates online grid strength estimation (eSCR), multi-scale tuning—slow-adaptation for virtual inertia/damping/droop and fast-adaptation for impedance reshaping—as well as angle-aware current limiting and post-fault resynchronization. Stability verification is performed through passivity/sector-bounded certification and ISS Lyapunov, while multi-GFC coordination utilizes virtual <math>\Delta f/\Delta V</math> sharing. EMT and HIL evaluations under SCR 6→1.7, load step, and FRT 1-<math>\phi</math>/3-<math>\phi</math> (120–200 ms) scenarios show that AR-GFC reduces ROCOF by ~35–40%, increases nadir frequency by +0.1–0.2 Hz, accelerates settling by 30–35%, and reduces voltage overshoot by 25–30%. At FRT, current violations are limited to <math>\leq 20</math> ms around <math>\approx 100\%</math> without internal angle loss; phase margin increases by +20–25°, the 4–6 Hz resonance peak is eliminated, and power sharing errors shrink to <math> \Delta P ,  \Delta Q  \approx 3\text{--}4\%</math> while reducing <math>I^2t</math> by ~20% and curtailment by 12–18%. These results confirm that AR-GFC maintains robust and fault-tolerant grid-forming properties, making it suitable for adoption in high renewable penetration transmission networks.</p>
 <p>This work is licensed under a <a href="https://creativecommons.org/licenses/by/4.0/">Creative Commons Attribution 4.0 International License</a>.</p>	<p><b>Corresponding Author:</b>  <b>Rio Khalifa</b> Pembangunan Panca Budi University, Medan, Indonesia Email : <a href="mailto:rio@gmail.com">rio@gmail.com</a></p>

### INTRODUCTION

High penetration of renewable energy sources (PV/wind) changes the transmission network from inertia-rich to inertia-light, resulting in faster frequency/voltage deviations, complex controller interactions, and the network often operating in low short-circuit ratio (SCR) conditions that trigger oscillations and negative damping between converter units. Grid-forming converters (GFCs)—with independent voltage/frequency regulation (PLL-free) such as droop, VSM, or matching control—promise stability, but in practice are vulnerable to plant parameter uncertainty, rapid topology changes, fault ride-through current limiting limitations, and control resonances in multi-GFC operations across areas; static/offline tuning-based designs are often non-adaptive and demand conservative margins that sacrifice transient performance (ROCOF, nadir). The problem statement of this research is: how to design an adaptive and resilient GFC control architecture that online identifies grid strength

(eSCR) and plant uncertainty, resets virtual inertia/damping/droop parameters and virtual impedance to avoid resonance, maintains current limits without losing grid-forming properties during FRT, and ensures stability (small-signal and input-to-state) and multi-GFC coordination at high renewable penetration? Contributions/novelty: (i) an adaptive multi-scale control framework that combines a passively certified current/voltage inner-loop with a VSM-droop type power/frequency outer-loop powered by an online eSCR estimator + disturbance observer for in-situ tuning; (ii) angle-aware current limiting and post-fault resynchronization so that FRT does not damage internal angle synchronization; (iii) anti-resonance re-shaping through virtual impedance adaptation based on network impedance maps so that resonance peaks and negative damping between controllers are suppressed; (iv) stability assurance through passivity/sector-bounded certification and Lyapunov input-to-state compatible with the EMT model; and (v) area-level multi-GFC coordination (virtual  $\Delta f/\Delta V$  sharing) for proportional power sharing and thermal stress limitation. The main novelty lies in the fusion of online network identification + certified adaptive tuning so that the GFC remains grid-forming, robust, and fault-tolerant in a highly renewable transmission network without compromising power quality or device current limits.

## METHODS

This research methodology is built as an end-to-end pipeline that integrates EMT modeling, online network strength identification, stable adaptive tuning, and HIL/experimental validation. First, we model a power bridge-based grid-forming converter (GFC) with LCL/LL filters, DC-links, sensors and actuators, along with a passively designed current/voltage inner loop (PR/PI + voltage feedforward and anti-windup protection). The multi-bus transmission network model includes frequency-dependent line impedances, transformers, and dynamic loads, as well as cascaded short-circuit ratio (SCR) scenarios (strong→weak). Nonidealities (dead-time, ADC/PWM delay, current saturation) are included to ensure realistic transient response and current limits.

Second, we develop an online grid-strength estimator to obtain the effective SCR (eSCR) and equivalent impedance maps at the point of connection (PoC). The estimation is performed from the system's natural excitation or small-signal injection, with a Kalman/DO observer that extracts  $|Z(j\omega)|$  in the 5–200 Hz band and filters outliers. The estimation is updated periodically ( $\approx 100$ –200 ms) and serves as a reference for the fault/resonance early detection module that monitors ROCOF, voltage deviation, phase jumps, and 1–10 Hz/100–600 Hz spectral peaks. A lightweight detector (spectral features + logic/fuzzy) classifies the event as a transient FRT or control resonance to trigger the appropriate adaptation mode.

Third, we design multi-scale adaptation laws. Slow-adaptation ( $\approx 100$ –500 ms) re-tunes the virtual inertia, damping, and P-f/Q-V droop based on the eSCR, angle margin, and aggregated power/voltage error, with parameter projection and slew-rate constraints to maintain oscillation-free operation. Fast-adaptation ( $\approx 10$ –20 ms) re-shapes the virtual impedance (R-L/C) to smooth out resonance peaks and increase phase margins when the grid weakens or the topology changes rapidly. To maintain

grid-forming characteristics during faults, we incorporate angle-aware current limiting: when the current approaches the device limit, the voltage reference is corrected to the quadrature component so that the current is contained without losing internal angular synchronization; after the fault is cut off, post-fault resynchronization with an eSCR-based adaptive voltage/frequency ramp prevents phase jumps.

Fourth, stability is analytically proven. The inner loop is certified passive/positive real after impedance shaping; the outer loop (VSM/adaptive droop) is constrained within sector bounds, so that the GFC-network interconnection satisfies input-to-state stability (ISS) under limited parameter variations and disturbances. Closed Nyquist/Bode analysis is used to verify the phase/gain margins over the eSCR range and measurement delay (1–4 ms), while current/voltage criteria guarantee operation within the invariant set (device current limits, over/under-voltage).

Fifth, we establish multi-GFC coordination between locations via area-level signals (virtual  $\Delta f/\Delta V$  sharing). An adaptive droop sharing scheme ensures proportional P/Q allocation of each unit's thermal capacity and  $I^2t$  limits, with rate-limiting of set-point changes to prevent simultaneous actions that induce hunting. This mechanism is integrated with circulating/reactive power management to dampen inter-controller interactions at 4–6 Hz that are common in low-SCRs.

Sixth, the test protocol includes nominal (load step, reactive bank switching), low-SCR (1.7–3), FRT (1- $\phi$ /3- $\phi$ , 120–200 ms, near/far), control resonance (LCL/delay variation), and multi-GFC (2–5 units across areas). Each scenario is run on baseline (fixed parameters), robust-fixed (conservative tuning), and the proposed method. Key metrics: ROCOF, nadir/overshoot & settling frequency/voltage, peak/duration current >100%, phase/gain margin, resonance index (Bode peak), THD/flicker, P/Q curtailment, and thermal stress ( $I^2t$ ). Ablation disables the eSCR estimator, fast impedance-shaping, angle-aware current limit, and area coordination to disentangle the relative contributions.

Seventh, implementation was conducted on a real-time platform (HIL/RTDS/OPAL-RT): inner loop 10–20 kHz, outer loop 1–5 kHz, eSCR estimator 5–10 Hz, with separate threading and documented latency budget. Adaptive parameters were assigned slew rates and bounds derived from stability evidence, while a dead-reckoning failsafe (conservative droop) was activated in the event of an extreme eSCR drop or sensor failure. Finally, laboratory prototype validation (5–20 kVA) replicated key scenarios to measure current/voltage, internal angle, and adaptive tuning response, and compared with EMT/HIL results. All configurations (YAML), eSCR estimation scripts, disturbance scenarios, and result data (CSV) were released for reproducibility and ready translation into utility practice.

## RESULTS AND DISCUSSION

### Quick Setup and Comparison

The evaluation is conducted on a multi-bus EMT model (110–220 kV equivalent) with 70–90% PV/wind penetration and four SCR levels: 6 (strong), 3 (medium), 2 and 1.7 (weak). Three schemes are tested: Baseline (fixed VSM/droop), Robust-Fixed (worst-point conservative tuning), and the proposed Adaptive-Resilient GFC (AR-GFC) method: online eSCR estimator, fast impedance reshaping (10–20 ms), angle-aware

current limiting, post-fault resynchronization, and multi-GFC coordination. The scenarios include  $\pm 10\text{--}20\%$  load stepping, reactive bank switching, 1- $\phi$ /3- $\phi$  faults 120–200 ms (near & far), synchronous unit shedding, and multi-GFC operation (2–5 units) across an area.

### **Frequency/Voltage Response (Nominal & Low-SCR)**

At SCR=3, AR-GFC decreases ROCOF by  $-36\text{--}40\%$  on average and increases frequency nadir by  $+0.12\text{--}0.18$  Hz compared to Baseline; frequency settling improves from 6.1 s  $\rightarrow$  3.9 s ( $-36\%$ ). Voltage overshoot decreases by  $-25\text{--}30\%$  and voltage settling decreases by  $\sim 33\%$  (2.7 s  $\rightarrow$  1.8 s). At SCR=1.7, Baseline shows 2–3 Hz oscillations ( $\zeta \approx 0.08$ ). With impedance reshaping, damping increases ( $\zeta \approx 0.23$ ), phase margin increases by  $+20\text{--}24^\circ$ , and peak Bode index decreases from  $+5$  dB  $\rightarrow$   $-1\text{--}2$  dB.

Interpretation: the combination of slow-adaptation (inertia/damping/droop adjustment) and fast-adaptation (virtual R-L/C) provides damping space that follows the eSCR changes online, so that transient performance is maintained on a weakened grid.

### **Fault Ride-Through (FRT) & Current Limit**

For a 150 ms 3- $\phi$  fault on the near bus (SCR=2), Baseline violates the current limit (110–118% for 40–60 ms) and triggers derating. AR-GFC holds the peak at 98–103% for  $\leq 20$  ms thanks to angle-aware current limiting that maintains the GFC's internal angular synchronization (without angle loss). After the fault is disconnected, eSCR-based post-fault resynchronization avoids phase jumps; voltage-dip recovery reaches  $>0.9$  pu in  $\sim 180\text{--}230$  ms,  $\approx 25\%$  faster than Robust-Fixed.

Practical significance: angle-aware current limiting prevents the GFC from switching to grid-following mode during current peaks, so that the grid-forming properties remain intact during the FRT.

### **Intercontroller Interaction & Resonance**

Multi-GFC operation ( $4 \times 100$  MVA equivalent) causes negative damping at 4–6 Hz when the power factor shifts (0.98 lag  $\rightarrow$  1.00). AR-GFC triggers rapid reshaping so that the resonance peak drops from  $>+5$  dB  $\rightarrow$   $-2$  dB and the phase margin increases from  $24^\circ \rightarrow 47^\circ$ . Reactive current hunting disappears and power sharing is stable.

### **Multi-GFC Coordination and Power Sharing**

With virtual  $\Delta f/\Delta V$  sharing and adaptive droop sharing, the active power sharing error  $|\Delta P|$  between units decreases from  $\pm 10.5\% \rightarrow \pm 3.2\%$ , and  $|\Delta Q|$  from  $\pm 12.8\% \rightarrow \pm 4.1\%$  at  $+15\%$  load step (SCR 2–3). The thermal stress ( $I^2t$ ) per unit decreases by  $\approx -22\%$ , which indicates a longer equipment life.

## Ablation Study

Variants	ROCOF (Hz/s) ↓	Nadir $\Delta f$ (Hz) ↑	V-overshoot (%) ↓	Current >100 % (ms) ↓	Phase Margin (°) ↑
Baseline (fixed)	0.72	+0.00	7.9	58	24
+ eSCR estimator only	0.64	+0.05	6.8	47	31
+ Adaptive virtual impedance	0.53	+0.10	5.4	36	41
+ Angle-aware current limit	0.53	+0.10	5.4	19	41
AR-GFC (complete)	0.45	+0.16	5.0	18	47

## Sensitivity, Robustness, and Limitations

The eSCR range is stable up to 1.6–1.7; below that, the system remains stable but nadir deteriorates ( $>0.25$  Hz) unless the ramp-rate is tightened and damping is increased. A measurement delay of 1–2 ms + 0.5 ms jitter is still safe; a delay of  $>4$  ms reduces the phase margin by  $\sim 6$ – $8^\circ$ . An LCL misestimation of  $\pm 15\%$  is tolerated by the projected adaptive law; an error of  $>25\%$  requires fast autocalibration. Limitations: at eSCR  $<1.5$  and large-area communication latency, stricter rate-limiting and system-level coordination (AGC/voltage control) are required.

## HIL/RT Validation & Prototype

At HIL/RT (inner 20 kHz; outer 2 kHz), the results are in line with EMT: ROCOF drops  $-34\ldots-39\%$ , V overshoot  $-24\ldots-29\%$ , and current  $>100\%$  is cut to  $\leq 20$  ms. The 10 kVA prototype with a 1- $\phi$  fault of 120 ms shows a peak current of  $\approx 101\%$  for  $<15$  ms and a recovery of 0.92 pu @ 210 ms, with no angle loss, consistent with the simulation.

## Practical Implications

AR-GFC enables high-RES operation with healthier stability margins without extreme tuning, suppresses derating during FRT, lowers  $I^2t$  and curtailment ( $-12\ldots-18\%$ ), and maintains THD  $\leq 1.5\%$  and lower flicker. Integration into utility practices benefits from stability certification (passivity/ISS) and clear parameter bounds.

## CONCLUSION

This study demonstrates that the Adaptive-Resilient GFC (AR-GFC) framework combining online eSCR estimation, multi-scale tuning (slow-adaptation for inertia/damping/droop and fast-adaptation for impedance reshaping), angle-aware current limiting and post-fault resynchronization is capable of maintaining grid-forming properties while improving performance and reliability in high-RES transmission networks. Compared to baseline and robust-fixed, AR-GFC consistently:

reduces ROCOF by ~35–40%, improves nadir frequency by +0.1–0.2 Hz, accelerates settling by 30–35%, reduces voltage overshoot by 25–30%, and limits current violations to  $\leq 20$  ms during FRT. In multi-GFC operation, this method increases the phase margin by +20–25°, dampens the 4–6 Hz resonance peak, stabilizes power sharing ( $|\Delta P|$ ,  $|\Delta Q| \approx 3\text{--}4\%$ ), and reduces thermal stress ( $I^2t$ ) by ~20% and curtailment by 12–18%. Performance remains robust at low-SCR ( $\approx 1.7$ ) and moderate latency, although for  $eSCR < 1.5$ , tighter rate-limiting and system-level coordination are required. In the future, the integration of fast auto-calibration, communication-aware area-level coordination, and long-term utility-scale validation will further strengthen the application of AR-GFC in high-renewable-penetration grids.

## REFERENCES

- [1] Zhong, Q.C., & Weiss, G. (2011). Synchronverters: Inverters That Mimic Synchronous Generators. *IEEE Transactions on Industrial Electronics*, 58(4), 1259–1267.
- [2] Arghir, C., Jouini, T., & Dörfler, F. (2018). Grid-forming control for power converters based on matching of synchronous machines. *Automatica*, 95, 273–282.
- [3] Unruh, P., Nuschke, M., Strauß, P., & Welck, F. (2020). Overview on Grid-Forming Inverter Control Methods. *Energies*, 13(10), 2589.
- [4] Sun, J. (2011). Impedance-Based Stability Criterion for Grid-Connected Inverters. *IEEE Transactions on Power Electronics*, 26(11), 3075–3078.
- [5] Musca, R., Vasile, A., & Zizzo, G. (2022). Grid-forming converters: A critical review of pilot projects and demonstrators. *Renewable & Sustainable Energy Reviews*, 165, 112551.
- [6] Taul, M.G., Wang, X., Davari, P., & Blaabjerg, F. (2020). Current Limiting Control with Enhanced Dynamics of Grid-Forming Converters during Fault Conditions. *IEEE Journal of Emerging and Selected Topics in Power Electronics*, 8(2), 1062–1073.
- [7] Qoria, T., Gruson, F., Colas, F., Kestelyn, X., & Guillaud, X. (2020). Current limiting algorithms and transient stability analysis of grid-forming VSCs. *Electric Power Systems Research*, 189, 106726.
- [8] Arasteh, A., Zeni, L., & Cutululis, N.A. (2022). Fault ride-through capability of grid-forming wind turbines: A comparison of three control schemes. *IET Renewable Power Generation*, 16(5), 1041–1056.
- [9] Dadjo Tavakoli, S., Ghahremani, A., Egea-Álvarez, A., & Gomis-Bellmunt, O. (2023). Fault ride-through control based on voltage prioritization for grid-forming converters. *IET Renewable Power Generation*, 17(10), 1370–1384.
- [10] Baekeland, N., Chatterjee, D., Lu, M., Johnson, B.B., & Seo, G.-S. (2024). Overcurrent Limiting in Grid-Forming Inverters: A Comprehensive Review and Discussion. *IEEE Transactions on Power Electronics*, 39(11), 14493–14517.
- [11] Shuai, Z., Shen, C., Liu, X., Li, Z., & Shen, Z. J. (2019). Transient Angle Stability of Virtual Synchronous Generators Using Lyapunov's Direct Method. *IEEE Transactions on Smart Grid*, 10(4), 4648–4661. (DOI recorded in IEEE Xplore).
- [12] Pan, D., Wang, X., Liu, F., & Shi, R. (2020). Transient Stability of Voltage-Source

- Converters With Grid-Forming Control: A Design-Oriented Study. *IEEE Journal of Emerging and Selected Topics in Power Electronics*, 8(2), 1019–1033.
- [13] Wu, H., & Wang, X. (2020). A Mode-Adaptive Power-Angle Control Method for Transient Stability Enhancement of Virtual Synchronous Generators. *IEEE Journal of Emerging and Selected Topics in Power Electronics*, 8(2), 1034–1049.
- [14] Xiong, X., Wu, C., & Blaabjerg, F. (2022). Effects of Virtual Resistance on Transient Stability of Virtual Synchronous Generators Under Grid Voltage Sag. *IEEE Transactions on Industrial Electronics*, 69(5), 4754–4764.
- [15] Xu, Z., Zhang, N., Zhang, Z., & Huang, Y. (2023). The Definition of Power Grid Strength and Its Calculation Methods for Power Systems with High-Proportion Nonsynchronous-Machine Sources. *Energies*, 16(4), 1842.